

# UC Davis

## UC Davis Previously Published Works

### Title

Selective Neuronal Knockout of STAT3 Function Inhibits Epilepsy Progression, Improves Cognition, and Restores Dysregulated Gene Networks in a Temporal Lobe Epilepsy Model

### Permalink

<https://escholarship.org/uc/item/7rd5h3nm>

### Journal

Annals of Neurology, 94(1)

### ISSN

0364-5134

### Authors

Tipton, Allison E  
Del Angel, Yasmin Cruz  
Hixson, Kathryn  
[et al.](#)

### Publication Date

2023-07-01

### DOI

10.1002/ana.26644

Peer reviewed



Published in final edited form as:

*Ann Neurol.* 2023 July ; 94(1): 106–122. doi:10.1002/ana.26644.

## Selective neuronal knockout of STAT3 function inhibits epilepsy progression, improves cognition, and restores dysregulated gene networks in a temporal lobe epilepsy model

Allison E. Tipton<sup>1,#</sup>, Yasmin Cruz Del Angel<sup>2,#</sup>, Kathryn Hixson<sup>1</sup>, Jessica Carlsen<sup>3</sup>, Dana Strode<sup>3</sup>, Nicolas Busquet<sup>4</sup>, Michael H. Mesches<sup>3</sup>, Marco I. Gonzalez<sup>2</sup>, Eleonora Napoli<sup>2</sup>, Shelley J. Russek<sup>1,5,#</sup>, Amy R. Brooks-Kayal<sup>2,#,\*</sup>

<sup>1</sup>Graduate Program for Neuroscience, Center for Systems Neuroscience, Boston University, Boston, MA, USA

<sup>2</sup>Department of Neurology, University of California Davis School of Medicine, Sacramento, CA, USA

<sup>3</sup>Department of Pediatrics, University of Colorado School of Medicine, Aurora, CO, USA

<sup>4</sup>Department of Neurology, University of Colorado School of Medicine, Aurora, CO, USA

<sup>5</sup>Department of Pharmacology and Experimental Therapeutics, Boston University School of Medicine, Boston, MA, USA

### Abstract

**Objective:** Temporal lobe epilepsy (TLE) is a progressive disorder mediated by pathological changes in molecular cascades and hippocampal neural circuit remodeling that results in spontaneous seizures and cognitive dysfunction. Targeting these cascades may provide disease-modifying treatments for TLE patients. Janus Kinase/Signal Transducer and Activator of Transcription (JAK/STAT) inhibitors have emerged as potential disease-modifying therapies; a more detailed understanding of JAK/STAT participation in epileptogenic responses is required, however, to increase the therapeutic efficacy and reduce adverse effects associated with global inhibition.

**Methods:** We developed a mouse line in which tamoxifen treatment conditionally abolishes STAT3 signaling from forebrain excitatory neurons (nSTAT3KO). Seizure frequency (continuous *in vivo* electroencephalography) and memory (contextual fear conditioning and motor learning) were analyzed in wild-type and nSTAT3KO mice after intrahippocampal kainate (IHKA) injection

\*Corresponding author at: Department of Neurology, University of California, Davis, School of Medicine, Sacramento, CA, 95817; abkayal@ucdavis.edu.

Author Contributions

ARB-K, SJR, and MHM contributed to conception and design of the study, data analysis, and drafting the manuscript; AET, YCDA, KH, JC, DS, MIG, and NB contributed to the data acquisition and analysis; AET and EN contributed to drafting some of the text and preparing the figures; YCDA and EN contributed to some of the data analysis.

#Authors contributed equally

Conflicts of Interest

The authors do not have any conflicts of interest or commercial relationships related to the study.

as a model of TLE. Hippocampal RNA was obtained 24 h after IHKA and subjected to deep sequencing.

**Results:** Selective STAT3 KO in excitatory neurons reduced seizure progression and hippocampal memory deficits without reducing the extent of cell death or mossy fiber sprouting induced by IHKA injection. Gene expression was rescued in major networks associated with response to brain injury, neuronal plasticity, and learning and memory. We also provide the first evidence that neuronal STAT3 may directly influence brain inflammation.

**Interpretation:** Inhibiting neuronal STAT3 signaling improved outcomes in an animal model of TLE, prevented progression of seizures and cognitive co-morbidities while rescuing pathogenic changes in gene expression of major networks associated with epileptogenesis. Specifically targeting neuronal STAT3 may be an effective disease-modifying strategy for TLE.

### Keywords

contextual fear conditioning; hippocampus; IHKA mouse model; RNA-sequencing; kainic acid; seizures; STAT3; temporal lobe epilepsy; tamoxifen; transcriptome; inflammation; synaptic plasticity

---

### Introduction

Temporal lobe epilepsy (TLE) is the most common form of focal epilepsy, affecting approximately 615,600 people in the United States.<sup>1</sup> TLE develops following a phase of epileptogenesis including molecular and structural changes, cell death, axonal sprouting, altered synaptic transmission, and inflammation, resulting in a brain overly susceptible to spontaneous seizures.<sup>2-5</sup> Although currently available medications for epilepsy can control seizures in approximately 65% of patients, they neither target epileptogenic processes underlying TLE nor modify the disease course. TLE is often a progressive disorder,<sup>6,7</sup> associated with cognitive and memory impairments that worsen over time.<sup>8</sup> Much like in the case of tuberous sclerosis complex (TSC), for which vigabatrin has shown promising in reducing risk and severity of epilepsy,<sup>9</sup> identifying the mechanisms underlying TLE progression might provide targets for disease modification after epilepsy onset.

The Janus Kinase/Signal Transducer and Activator of Transcription (JAK/STAT) pathway plays a major role in the inflammatory response of microglia via cytokines/chemokines. Brain injuries leading to epilepsy, such as traumatic brain injury, stroke, and status epilepticus (SE), activate the JAK/STAT signaling pathway in the rodent brain.<sup>10-12</sup> Brain tissue resected from patients with intractable epilepsy also shows JAK/STAT activation.<sup>13</sup> In neurons, the JAK/STAT pathway regulates GABA<sub>A</sub> receptor subunit gene expression<sup>14-16</sup> as well as the transcription of multiple genes involved in neuronal plasticity and survival that are essential for normal brain function<sup>14</sup> and important contributors to epileptogenesis. Moreover, transient pharmacological reduction of JAK/STAT activation at the time of injury reduces the severity of subsequent epilepsy.<sup>10</sup> Although STAT3 signaling in microglia and astrocytes is implicated in the etiology of many brain disorders, including Alzheimer's disease, depression, and epilepsy,<sup>17-19</sup> the contribution of the neuronal STAT3 response to

epileptogenesis and inflammatory processes mediated by glia in response to brain injury is unknown.

To address this question, we used a novel mouse model in which functional knockout of STAT3 signaling is selectively induced in excitatory forebrain neurons, with no direct effect on STAT3 gene transcription in microglia or astrocytes. Utilizing the intrahippocampal kainate (IHKA) model of TLE, we examined whether selective loss of STAT3 function in excitatory neurons prevents development or progression of spontaneous seizures or impacts hippocampal memory and sensorimotor learning deficits typically observed in this model. To further clarify the specific role of STAT3 in epileptogenesis, we performed high-resolution RNA-sequencing to identify genes in the hippocampus whose expression was altered by IHKA and rescued by loss of functional forebrain neuronal STAT3.

## Materials and Methods

### Animals

Experiments were conducted in accordance with PHS Policy on Humane Care and Use of Laboratory Animals and approved by the University of Colorado IACUC. Adult C57BL/6J male mice were group-housed with up to 5 age- and sex-matched littermates in temperature and humidity-controlled rooms with access to food and water ad-libitum on a 14-h light/dark cycle. Breeding pairs of *B6.129S1-Stat3tm1Xyfu/J* (Stat3flox, Stock#: 016923) and C57BL/6J (WT) mice were acquired from the Jackson Laboratories (Bar Harbor, ME). Breeding pairs of *Tg(camk2a-cre/ERT2)2Gsc* mice were obtained from Dr. Günther Schütz, Heidelberg, Germany. Parental lines were backcrossed on a C57BL/6J background for >10 generations prior to being crossed to produce *camk2a-cre/ERT2/Stat3<sup>fl/fl</sup>* mice.

To knock-out STAT3 function in excitatory neurons (nSTAT3KO), tamoxifen (TX) was administered to *camk2a-cre/ERT2/Stat3<sup>fl/fl</sup>* mice at 7–8 weeks to delete exons 18–20 of *Stat3* (encoding the SH2 domain) in Camk2a-promoter-driven-Cre. TX was dissolved in corn oil (vehicle) at a concentration of 20 mg/ml; mice were injected intraperitoneally with 100 mg/kg/day for 5 days to induce recombination. Age-matched WT C57BL/6J mice were used as controls. Half of the mice of each group underwent intrahippocampal injections of kainate (IHKA) and the other half intrahippocampal injections of saline (IHSaline). To account for potential effects of TX alone, WT mice treated with TX (n=14) or vehicle (~100 µl oil, n=14) for 5 days were also examined. No significant difference (unpaired Student's t test) was detected between WT with or without TX for any parameters tested, and combined data was collectively labeled WT.

### Kainate-induced SE and electrode implantation

Two weeks after TX treatment (allowing time for STAT3 KO and resolution of any acute effects of TX-dependent estrogen blockade), isoflurane anesthetized mice were placed in a stereotax under normothermia. Burr holes (0.8 mm) were drilled over bilateral hippocampal CA1 region (depth electrodes, right intrahippocampal injection), frontal cortices (subdural electrodes), and caudal to lambda (reference and ground electrodes). KA or saline injections were targeted immediately dorsal to CA1 (2.0mm posterior to bregma, 1.3mm lateral from

midline, 1.5mm below dura). KA (20mM; 100nl, 2-min dwell time) dissolved in phosphate-buffered saline (PBS) was infused via infusion pump. Electrode assembly fixed with dental cement, anesthesia discontinued, electrodes connected to swivel commutator, and EEG recordings initiated. SE began within 15 min in all animals and motor seizures were scored as previously described.<sup>10</sup>

### Electroencephalography acquisition

Mice underwent continuous (24/7) video-EEG monitoring for 4 weeks using Pinnacle digital video-EEG systems. EEG was analyzed by investigators blinded to the genotype and treatment group, as previously described.<sup>10</sup>

### Behavioral assessment

Following 4-weeks of EEG recordings, mice were tested for associative memory and motor skill learning by investigators blinded to the genotype and treatment group. Contextual fear conditioning (CFC) was performed as previously described,<sup>22</sup> with modifications. Mice were placed in conditioning boxes (Med-Associates, Fairfax, VT) for 7 min on days 1 and 3. On day 1, foot shock (0.7mA, 2s constant current; unconditioned stimulus-UCS) was delivered at 148s and 298s. Freezing was defined as the lack of movement (except required for respiration) for 2s. On day 3, memory for context was evaluated by placing animals back in test chamber, and freezing evaluated in the presence of context but not UCS. Freezing quantified using FreezeScan software (Clever-Sys, Reston, VA), and immobility time used as measure of learning/memory performance. Rotarod test was used to measure motor coordination<sup>20</sup> and sensorimotor skill learning, as described previously.<sup>21</sup>

### Immunohistochemistry

*Fluoro-Jade C (FJC)* WT and nSTAT3KO mice were transcardially perfused with 4% paraformaldehyde in ice-cold PBS 48 h after IHKA-induced SE, post-fixed overnight, then cryoprotected in 30% sucrose. Frozen whole brains embedded in Tissue-Plus O.C.T. medium (ThermoFisher-Scientific) were serially sectioned (14  $\mu$ m) in coronal plane. Sections were processed as previously described<sup>10</sup> and analyzed using NikonEclipse TE2000-U fluorescence microscope 10–20x magnification by investigator blinded to genotype and treatment. FJC-positive cells were counted within standardized areas of the CA1, CA3, and hilar regions of hippocampus using ImageJ software (v.1.53a).

*NeuN*, *VGLUT1*, *ZnT3* WT and nSTAT3KO mice were perfused >30 days after intrahippocampal injection, and brains were processed as above. Slides dried 20 min at RT, PBS washed 3 $\times$ 5 min and antigen retrieval performed in sodium citrate buffer (10 mM Na<sub>3</sub>C<sub>6</sub>H<sub>5</sub>O<sub>7</sub>, 0.05% Tween-20; 10 min@95°C then 30 min@RT), followed by 3-PBS washes and blocking with 10% normal goat serum (NGS; Vector Labs) in PBST (0.3% Tween 100/PBS) for 1 h. Slides incubated overnight in anti-NeuN (#MAB377, Millipore; 1:600), anti-VGLUT1 (#AGC-035, Alomone; 1:400), or anti-ZnT3 (#197–002, Synaptic Systems; 1:500) primary antibody in 7.5%-NGS/0.3%-PBST, washed 3 $\times$ 5 min in PBS, incubated in AlexaFluor568 goat-anti-mouse (#A11031, Invitrogen; 1:800) or AlexaFluor488 goat-anti-rabbit (#A11034, Invitrogen; 1:600) secondary antibody for 1 h, washed in PBS 3 $\times$ 5 min, and mounted using Vectashield media/DAPI (#H1200, Vector Labs).

### RNA extraction protocol

RNA was extracted from hippocampi numerically labeled without treatment designation and bulk RNA-sequencing was performed using 500 µl Qiazol for tissue homogenization with the Qiagen RNeasy mini kit. RNeasy mini columns were used to purify RNA and remove DNA using DNase I (Cat.#74804). Quantity and quality of RNA were verified via Bioanalyzer (Agilent-2100).

### RNA library preparation and sequencing

**Preparation**—The NEB Next rRNA depletion kit (E6310) was used for RNA purification, as several samples had RNA integrity numbers <8 (but >7). Most samples had RNA integrity numbers >8. After rRNA depletion, the NEBNext UltraII Directional Kit (E7765) and NEB Multiplex Oligos (Kits-E7335,E7710) were used to generate and barcode sample libraries. Library concentrations were quantified by quantitative polymerase chain reaction using KAPA Quant assays, and values were used to generate an equimolar pool to ensure equal distribution of reads across all samples.

**RNA sequencing**—Three hippocampi from each condition were used. RNA libraries (one per sample) from nSTAT3KO mice and WT mice were pooled separately (run together on the sequencer in equimolar concentration, to help avoid sequencer-based batch effects that could potentially conflate biological effects), blinded by treatment group, and read deeply (70–80 million reads/sample) using the NextSeq 500 Illumina system (Harvard Biopolymers Facility).

### Bulk RNA-sequencing analysis

Data analysis performed using Partek Flow. Following QA/QC checks of FastQ files to assess for sequencing errors, adapter sequences were trimmed from reads, and reads were aligned to mouse genome build GRCm38/mm10 using STAR. Aligned reads were subsequently quantified to mm10 RefSeq Transcripts-95, generating gene-level counts per gene across all samples. DESeq2(R) version 3.5 was employed to normalize count data and calculate differentially expressed genes (DEGs) between groups (hypothesis test: Wald, FDR=<0.05).

### Downstream RNA-sequencing analysis

DEGs (differentially expressed genes with fold change  $\geq 1.5$ , FDR=<0.05) from DESeq2 were used for downstream enrichment analysis. Databases/programs used to elucidate key pathways and processes impacted by IHKA and rescued in nSTAT3KO mice were: Ingenuity pathway analysis (IPA), curated database of literature findings for transcriptomic/proteomic data that identifies canonical pathways, upstream regulators, and disease and functional associations enriched in datasets (importantly, IPA incorporates directionality and degree of change between conditions, allowing for functional predictions); enrichR, web- and code-based program that carries out enrichment analysis for an uploaded gene list across dozens of databases, including GO, KEGG, and Reactome; and Metascape, allowing for parallel comparison of numerous gene lists to identify shared expression patterns and functional enrichment when there are multiple conditions in an experiment. Certain processes or

pathways identified by gene enrichment analysis are referred to as “rescued” after nSTAT3 KO in the IHKA model dependent on whether all genes, or the majority of them, are no longer found within the corresponding gene list. Likewise, processes or pathways that are “partially rescued” represent those where only a portion of the genes are absent indicating that the pathway is still engaged but at a predicted lower level.

### Statistical analysis

A mixed effect model (REML) 2-way ANOVA followed by Šídák’s or Tukey’s post-hoc tests was used for the analysis of SRS data. Fisher’s exact test was used to compare proportions of motor and nonmotor seizures. Rotarod and CFC data were analyzed with Kruskal-Wallis test followed by uncorrected Dunn’s post-hoc. Distribution of datasets was evaluated by the D’Agostino-Pearson normality test. GraphPad Prism software (version 9.3.1) used for analysis.

## Results

### Spontaneous recurrent seizure frequency and epilepsy progression in nSTAT3KO mice

IHKA injection resulted in highly consistent development of spontaneous electrographic and electroclinical seizures in all animals with negligible mortality. In the 4 weeks post-IHKA injection, the total number of spontaneous recurrent seizures (SRS) was significantly lower in nSTAT3KO than WT (Fig 1A). Remarkably, nSTAT3KO mice did not exhibit the progressive time-dependent increase in seizures observed in WT; marked intergroup differences in seizures/week began at week 3 post-IHKA (Fig 1B, 1C). No significant difference was detected between WT and nSTAT3KO in proportion of motor-to-nonmotor seizures (Fig 1D), mean latency to spontaneous seizure onset or seizure duration and severity (Fig S1A–C). SE duration and intensity were unaffected by nSTAT3 KO, as indicated by comparable EEG integrated power at multiple bandwidths, maximum power, and SE duration (time from maximum power to 20% power)<sup>10</sup> in both groups (Fig S1D–F).

These findings suggest that inhibition of the JAK/STAT pathway through functional nSTAT3 KO affects the frequency and progression of SRS, but not SE severity, magnitude, or duration. Thus, differences in the initial injury severity (SE) are unlikely to account for differences in seizure frequency/progression of SRS between groups. Importantly, the total post-IHKA seizure number did not differ significantly between TX-treated and vehicle-treated WT, indicating that TX treatment ending 2 weeks prior to IHKA had no effect on seizure development or progression in WT mice (Fig S2).

### Sensorimotor skill learning is impaired in epileptic WT but not nSTAT3KO mice

The rotarod was used to assess the impact of SE on motor skills acquisition and learning. WT and nSTAT3KO mice with or without IHKA were tested in 3 trials. To exclude the contribution of coordination and balance differences related to body mass variability across groups, Trial 3 latencies were normalized by values recorded in Trial 1, providing a measure of motor skill learning (Fig 1E). Mean values calculated for nSTAT3KO with or without IHKA were not different from WT control values, suggesting that motor learning was not impaired in either control or epileptic nSTAT3KO mice. Conversely, normalized Trial 3

latency in IHKA-WT was 56% that of control WT values (Fig 1E), suggesting impaired motor skill learning in epileptic WT mice.

### **Reduced hippocampal associative memory in epileptic WT but not nSTAT3KO mice**

CFC was utilized to assess hippocampal memory 6 weeks after IHKA injection. On day 1, mice in all groups exhibited an increase in freezing response between the first 2 min (baseline) and the 2 min after exposure to foot shock [UCS]. When tested 48 h later in the same setting used in day 1, but without UCS, WT sham, and both nSTAT3KO groups ( $\pm$  IHKA injection) showed levels of freezing behavior at or above those seen after UCS on day 1, demonstrating memory of the context. In contrast, IHKA-WT mice exhibited decreased freezing relative to their response to UCS, indicating impaired memory for context only in the epileptic WT mice (Fig 1F).

Differences in freezing behavior recorded among groups on day 1 (increased freezing in response to UCS in both IHKA groups and nSTAT3KO sham relative to WT sham after UCS) may reflect underlying differences in anxiety or activity levels (inactivity cannot be differentiated from freezing in this task). In addition, due to the known link between hippocampal STAT3 signaling and leptin regulation on metabolic function,<sup>22</sup> nSTAT3KO mice had significantly greater body weight relative to WT, which may have impacted overall activity. However, the comparison between sham and their IHKA-treated counterpart accounted for the contribution of body weight on the intra-group freezing behavior for both WT and nSTAT3KO mice.

### **STAT3 KO does not affect IHKA-dependent neuronal cell death or density in hippocampus**

Several STAT3-target genes previously identified in a pilocarpine rat model of acquired epilepsy are implicated in apoptosis.<sup>10</sup> Hence, immunohistochemistry was conducted to determine whether STAT3 KO altered cell death levels in the hippocampus in response to IHKA-induced SE. Fluoro-JadeC (FJC), an anionic fluorochrome used to selectively probe degenerating neurons,<sup>10, 23, 24</sup> was used to stain coronal sections of the CA1, CA3, and dentate hilus ipsilateral to the IHKA injection site from vehicle and TX-treated mice sacrificed 48 h post-SE (Fig 2A, 2B). Consistent with our previous findings in rats,<sup>10</sup> no significant difference in FJC-staining was observed in any of the hippocampal regions of nSTAT3KO mice compared with WT mice (Fig 2A, 2B), indicating that nSTAT3KO did not affect the amount of overall acute hippocampal cell death after IHKA SE. No difference in the FJC-positive cell number was detected between TX- and oil-treated IHKA WT (Fig 2A, 2B), confirming that TX treatment does not affect neuronal degeneration.

NeuN (a postmitotic neuronal marker) was used to quantify neurons in ipsilateral CA1 and CA3 in TX-treated WT and nSTAT3KO mice 30 days after either saline or KA injection (Fig 2C, 2D). IHKA produced a significant reduction in NeuN-positive cells in WT and nSTAT3KO mice in both regions. As expected, the contralateral CA1 or CA3 was not affected (Fig S3). To assess whether specific STAT3 KO might affect cell death selectively in excitatory neurons, we performed immunofluorescent staining of the vesicular glutamate transporter 1 (VGLUT1; Fig 2E, 2F), a marker of glutamatergic neurons.<sup>25–27</sup> Mirroring the results obtained for NeuN, a comparable and significant IHKA-dependent reduction in the

number of VGLUT1-positive cells was noted in ipsilateral CA1 and CA3 of both WT and nSTAT3KO (Fig 2E, 2F).

Taken together, these data suggest that IHKA-induced SE results in a substantial hippocampal neuronal loss that is neither rescued nor exacerbated by neuronal STAT3 functional knockout.

### **SE-induced mossy fiber sprouting is not altered in STAT3 KO mice**

To visualize mossy fiber sprouting in the dentate gyrus inner molecular layer, a hallmark of TLE in both animals and humans,<sup>28, 29</sup> coronal sections from WT and nSTAT3KO mice 5–6 weeks post-IHKA were stained with an antibody against zinc transporter 3 (ZnT3), which is highly enriched in mossy fiber terminals.<sup>30</sup> Saline-injected mice, regardless of the genotype, showed negligible ZnT3 staining (Fig 2G, 2H), while KA-induced SE resulted in a marked and comparable staining increase in both WT and nSTAT3KO mice.

### **Transcriptomic responses to IHKA injection in WT mice**

At 24 h-post injection, 3190 genes were differentially expressed in WT mice injected with KA vs saline (fold change  $\geq 1.5$ , FDR $\leq 0.05$ ). IPA revealed significant enrichment in 2 overarching sets of pathways: 1) those related to synaptic signaling and 2) those related to inflammation (Fig 3A). As expected, many of the IHKA-induced genes were previously associated with epilepsy or seizures disorders (260 for Seizure Disorder, 267 for Epilepsy or Neurodevelopmental Disorder), and Seizure Disorder had the highest activation score in Neurological Disease based on gene expression patterns (Fig S4). Interestingly, a closer analysis of the IHKA-induced gene set revealed an enrichment of STAT3-associated genes (216), most of which were upregulated by IHKA (Fig 3B).

### **Rescue of the transcriptome in nSTAT3KO mice**

To examine what gene changes may be involved in phenotypic rescue in nSTAT3KO mice, gene expression in IHKA-injected WT mice and IHKA-injected nSTAT3KO mice were assessed against the same control, gene expression in saline-injected WT mice. Compared to the 3190 Differentially Expressed Genes (DEGs) between IHKA and saline-injected WT mice 24 hours after SE, more than half of these DEGs (1609) were rescued when comparing IHKA-injected nSTAT3KO mice and saline-injected WT mice (Circos plot, Fig 3C), indicating a significant rescue of gene expression when nSTAT3 is absent.

Lists of DEGs between saline and IHKA conditions were entered into IPA to identify the top canonical pathways that may be rescued by nSTAT3 KO. Many of these pathways relate to the genes already associated with seizure disorder (Fig 4A) and the IHKA-induced inhibition of neuronal functions [such as long-term depression (LTD), synaptogenesis, opioid signaling, endocannabinoid neuronal synapse pathway, and neurovascular coupling; Fig 4B]. Concurrent enrichment analyses of gene sets from IHKA-induced WT and nSTAT3KO mice (using Metascape) showed that many of the enriched pathways and processes in genes rescued by nSTAT3 KO are common to some of the most enriched pathways amongst IHKA-induced genes (Fig 4C). This suggests that nSTAT3 manipulation has a profound impact on transcriptomic response to seizures.

To dissect the potential impact nSTAT3 might play in epilepsy patients, we looked at the specific aspects of inflammation rescued with nSTAT3 KO using the WikiPathway 2021 Human Database (Fig 5A). A potential rescue of interferon signaling was identified, which was not surprising as STAT proteins, including STAT1 and STAT3, participate in upregulation of interferon regulatory factors,<sup>31, 32</sup> which themselves serve as transcription factors for interferon responsive genes. Indeed, nSTAT3 KO reversed the upregulation of many genomic targets of the interferon signaling pathway (Fig 5B).

Similarly, the change in gene expression following IHKA was predicted to increase microglia-dependent migration and phagocytic function in WT but not nSTAT3KO (Figs 5C, 5D), an unexpected finding since STAT3 KO occurs only in excitatory neurons.

### Predicted rescue of processes related to synaptic function

Given that IHKA-injected nSTAT3KO mice not only develop fewer seizures, but also perform better in contextual fear conditioning than their WT counterparts, we wondered whether nSTAT3 KO also rescued DEGs related to synaptic function. Results from enrichment analysis using the Bioplane 2019 Database through EnrichR indicate that nSTAT3 KO rescues IHKA-altered genes relevant to neurotransmission and nervous system functioning, including calcium signaling, neurotransmitter release, and GABA cycling (Fig 6A). Enrichment analysis via GO Cellular Components provides additional support for rescued DEGs relevant to neuronal signaling (Fig 6B), as most of the top enriched compartments relate to connections between cell types (including neurons) or compartments relevant for communication between neurons (e.g., synaptic vesicle membrane). nSTAT3 KO is also associated with IHKA-induced downregulation of multiple transcripts coding for GABA<sub>A</sub> receptor (GABAR) subunits and GABA transporters (Figs 4A, 6C).

Alterations in gene expression 24 h post-IHKA also support decreased neuritogenesis compared to saline controls, which nSTAT3 KO partially reverses (Fig 7A). While decreases in neuritogenesis and other processes related to neuronal signaling may be a protective response in the immediate aftermath of SE, sustained suppression of neuritogenesis may explain learning and memory impairments observed at 4 weeks in the IHKA model, and the rescue of those impairments in nSTAT3KO mice (Fig 1). Indeed, further examination of genes rescued by nSTAT3 KO support a reversal of IHKA-induced alterations in gene expression associated with decreased learning (Fig 7B), as well as the related but distinct function of memory (Fig 7C).

## Discussion

Over one-third of adults with epilepsy have inadequate seizure control despite the introduction of more than a dozen new antiseizure medications in the last 2 decades. TLE is often a progressive disorder.<sup>6</sup> Although seizures may initially respond to medication, intractability develops over ~9 years, and cognitive and memory impairments worsen as the disease progresses.<sup>7,8</sup> Identifying the mechanisms underlying TLE progression may elucidate targets for disease modification after epilepsy onset, which would be clinically beneficial considering that most patients seek clinical attention after seizure onset, as initial precipitating events are typically identified retrospectively.

Systemic inhibition of STAT3 activation reduces the number of spontaneous seizures in a rat pilocarpine-TLE model,<sup>10</sup> but the adverse effects (immunosuppressant, gastrointestinal, metabolic, and cardiac) of systemic STAT3 inhibition limit its potential clinical utility. Several basic mechanisms by which STAT3 promotes epileptogenesis, such as mediating  $\alpha 1$  subunit-GABAR downregulation on the neuron surface,<sup>15, 33</sup> relate to its neuronal activity, suggesting that specifically targeting neuronal STAT3 inhibition could be an effective and safe disease-modifying strategy. Reduced  $\alpha 1$ -GABA<sub>A</sub> gene expression is linked to epilepsy in both humans and rodents,<sup>15, 34, 35</sup> as well as to other nervous system disorders.<sup>36, 37</sup> A non-canonical brain-derived neurotrophic factor-induced JAK/STAT signaling pathway (not relying on STAT3 phosphorylation at Y705) with a unique transcriptional role in regulating the brain's most essential ion channels and neurotransmitter receptors was identified in primary neurons.<sup>14</sup>

Here, we examined the effects of impaired nSTAT3 signaling on epileptogenesis and seizure progression in the IHKA model of TLE using STAT3 floxed *Camk2a-Cre-ERT2* expressing mice treated with TX to induce deletion of exons 18–20 of *Stat3* leading to the translation of a functionally inactive form of STAT3 exclusively in *Camk2a* promoter-driven Cre-expressing excitatory neurons.<sup>38</sup> The IHKA model of TLE recapitulates the temporal lobe damage,<sup>39–41</sup> histological changes,<sup>39, 40, 42</sup> and deficits in hippocampal-dependent memory characteristic of human TLE.<sup>39–41, 43–45</sup> Although we detected no difference in the severity or length of KA-induced SE between WT and nSTAT3KO mice, there was a >3-fold reduction in the total number of SRS in nSTAT3KO mice. Remarkably, nSTAT3KO mice did not show the progressive increase in seizures seen in WT during >4 weeks of recording. In this regard, while the contribution of an anticonvulsant effect secondary to STAT3 KO cannot be ruled out, our previous pharmacological studies in the pilocarpine model of acquired epilepsy show that brief exposure to a systemic pharmacological inhibitor of the JAK/STAT pathway early after the onset of SE suppresses spontaneous seizure frequency via inhibition of STAT3-regulated transcription of genes (*mcl-1*, *bcl-2*, *bcl-xl*, *c-myc*, *cyclin D1*, *VEGF*) implicated in pathological processes that may be important to epileptogenesis.<sup>10</sup> This suggests that long term inhibition of STAT3 has at least some antiepileptogenic effect that could contribute to a reduction of SRS. This claim is supported by the findings of our current study, which point to potentially long-term STAT3-dependent effects on GABA<sub>A</sub> gene expression as well as on the transcription of multiple genes involved in neuronal plasticity and survival that are essential for normal brain function and important contributors to epileptogenesis.

Immunohistochemical studies of NeuN and VGLUT1 confirmed the KA-dependent loss in hippocampal CA1 and CA3 neurons ipsilateral to the injection site, with negligible cell death in contralateral regions. Consistent with our findings on pharmacological STAT3 inhibition in the pilocarpine model of acquired epilepsy,<sup>10</sup> nSTAT3 KO did not exacerbate or rescue the loss of excitatory neurons 30 days after IHKA injection. Further, nSTAT3 KO did not impact dentate granule cell (DGC) mossy fiber sprouting in the hippocampus, a phenomenon observed in mesial TLE in humans and thought to contribute to epileptogenesis by promoting generation and propagation of spontaneous seizure activity.<sup>46</sup> In our IHKA mouse model, mossy fiber sprouting was evident 6 weeks after SE induction, and occurred equivalently in both WT and nSTAT3KO mice, suggesting that it is not a nSTAT3

downstream effector, and that the observed progression of spontaneous seizures is not (or not exclusively) related to mossy fiber sprouting.

The acquisition of contextual fear memory depends in large part on the hippocampus-amygdala circuit in both humans and rodents.<sup>47–50</sup> In the CFC task, epileptic WT mice showed impaired hippocampus-dependent memory for context. Remarkably, this effect was not observed in epileptic nSTAT3KO mice, pointing to a critical role for STAT3 in memory formation specific to excitatory neurons. Similarly, decreased motor learning was observed in IHKA-WT mice during testing on the rotarod, but not in nSTAT3KO mice upon induction of SE. The rotarod is typically used to assess cerebellar deficits in rodents.<sup>51</sup> Recent studies, however, demonstrated that longer latencies on the rotarod are associated with increased hippocampal fractional anisotropy (a measure of connectivity in the brain) between the molecular and pyramidal layers of CA1, as well as an increased volume between the dentate gyrus and the molecular layer of CA1,<sup>52</sup> suggesting that the hippocampus is the most plastic brain area in response to rotarod training. Hence, it is not unexpected that hippocampal damage elicited by IHKA would lead to impaired motor learning skills in epileptic mice. The observation that selective STAT3 KO in excitatory neurons prevents such impairment suggests the intriguing possibility that STAT3-regulated glutamatergic transmission might also be involved in sensorimotor learning.

Given that IHKA-injected nSTAT3KO mice go on to develop fewer seizures, we were not surprised to find that many gene expression changes associated with increased likelihood of seizures were reversed in nSTAT3KO mice, supporting the idea that changes in gene expression observed just 24 h after SE are likely relevant to the modification of seizure number in the chronic stage of epilepsy. While nSTAT3 KO influences the expression of genes in many different pathways, including learning and memory, the greatest surprise came from the predicted regulatory control over microglial function. nSTAT3KO mice had the greatest number of DEGs in pathways that regulate inflammation and ion transport, and while inflammation was an expected response to IHKA, we were surprised to find evidence for its rescue in nSTAT3 KO mice.

In the context of inflammation, phagocytes are a particularly important class of first responders to injury, including the resident phagocytes of the brain, microglia. The response of phagocytes is essential to orchestrating a robust immune system response to injury or infection. While initial recruitment and activation of phagocytes is desired, and likely beneficial in the setting of an insult, it can also introduce additional local tissue damage in the setting of chronic inflammation. Our findings suggest that nSTAT3 KO reverses the predicted increased trafficking and phagocytic function of microglia. This is particularly intriguing because enrichment of DEGs related to microglial function occurs after STAT3 is exclusively knocked-out in excitatory neurons (Fig 8). Further studies using single-nuclei-RNA sequencing to directly identify cell types most affected by STAT3 KO in excitatory neurons are warranted to establish the time window during which functional changes in neuron excitability, morphology, and glial activation occur, and to clarify the sustainability of the changes in gene expression that may directly rely on nSTAT3 activation.

To our knowledge this is the first study directly implicating neuronal JAK/STAT signaling as a critical contributor to the development and progression of acquired epilepsy. Nevertheless, the current findings must be seen in light of some limitations: (i) Our model is a functional KO in which only a very small portion of the STAT3 protein is missing due to deletion of exons 18–20 of *Stat3* encoding the SH2 domain that is essential for STAT3 dimerization. While it would be ideal to demonstrate this, there are significant challenges to the feasibility of doing so at both the protein and mRNA level. This mutation does not change overall STAT3 protein expression levels, it only changes dimerization, and there are currently no commercially available antibodies that can differentiate between STAT3 dimers and monomers; (ii) Given the timeframe used for our EEG experiments (4 weeks), we cannot exclude the possibility that SRS may just have been delayed, rather than completely prevented, in KO animals; (iii) as we initially sought to test STAT3 target genes in excitatory neurons during early epileptogenesis, transcriptomic signatures were evaluated at only 24 h after IHKA rather than at later times when significant behavioral differences were recorded (4 weeks); finally (iv) while the IHKA model recapitulates behavioral, electrophysiological, and anatomical features of TLE, future studies are warranted to clarify the effect of STAT3 inhibition in a model that does not produce significant inflammation and neurotoxicity (as in the case of febrile seizures).

Future experiments are planned in our laboratory to address all these critical points. In particular we will assess the contribution of nSTAT3 to longer-term SRS frequency, and employ single cell RNA sequencing to identify sustained effects of nSTAT3-dependent gene expression in different cell types (excitatory and inhibitory neurons and glia).

Despite the limitations listed above, our novel findings suggest that neuronal STAT3 activity affects gene regulation in multiple pathways in different cell types involved in TLE development and progression. Targeting nSTAT3 through the development of selective inhibitors may lead to disease-modifying therapies that reduce TLE disease progression, are less toxic than current drugs with broad JAK/STAT inhibition across cell types and have greater efficacy to prevent cognitive comorbidities associated with epilepsy.

## Supplementary Material

Refer to Web version on PubMed Central for supplementary material.

## Acknowledgements

We thank the University of Colorado Anschutz Medical Campus NeuroTechnology Center's Animal Behavior and In Vivo Neurophysiology Core for providing facilities and equipment to acquire and analyze the animal behavior and video-EEG data. We also thank the Genome Science Institute at Boston University for the core sequencing award to AET and the generous advice from Director Yuriy Alekseyev and Joshua Campbell. We thank Dr. Danielle Harvey for her assistance with the statistical analysis of the SRS and behavioral data. Research reported in this publication was supported by the National Institute of Neurological Disorders and Stroke of the National Institutes of Health under Award Numbers R01NS051710, R56NS117141, R01NS122385, P30NS048154 and NIGMS T32 GM008541 for AET. The content is solely the responsibility of the authors and does not necessarily represent the official views of the National Institutes of Health. SciTechEdit International LLC (Highlands Ranch, CO) provided manuscript editing support.

## Abbreviations:

<b>CFC</b>	contextual fear conditioning
<b>CS</b>	conditioned stimulus
<b>DEGs</b>	differentially expressed genes
<b>DGCs</b>	dentate granule cells
<b>FJC</b>	Fluoro-Jade C
<b>EEG</b>	electroencephalography
<b>IACUC</b>	Institutional Animal Care and Use Committee
<b>IHKA</b>	intrahippocampal kainate
<b>IPA</b>	ingenuity pathway analysis
<b>KA</b>	kainate
<b>KO</b>	knock-out
<b>LTD</b>	long-term depression
<b>NeuN</b>	neuronal nuclei
<b>nSTAT3</b>	neuronal STAT3
<b>SE</b>	status epilepticus
<b>SRS</b>	spontaneous recurrent seizures
<b>TLE</b>	temporal lobe epilepsy
<b>TX</b>	tamoxifen
<b>US</b>	unconditioned stimulus
<b>VGLUT1</b>	vesicular glutamate transporter 1
<b>ZnT3</b>	zinc transporter 3

## References

1. Asadi-Pooya AA, Stewart GR, Abrams DJ, et al. Prevalence and Incidence of Drug-Resistant Mesial Temporal Lobe Epilepsy in the United States. *World Neurosurg* 2017;99:662–666. [PubMed: 28034810]
2. Berg AT. The natural history of mesial temporal lobe epilepsy. *Curr Opin Neurol* 2008;21:173–178. [PubMed: 18317276]
3. Buckmaster PS. Mossy fiber sprouting in the dentate gyrus. In: Noebels JL Avoli M, Rogawski MA, Olsen RW, Delgado-Escueta AV, editors. *Jasper's Basic Mechanisms of the Epilepsies*. 4th ed. Bethesda (MD): National Center for Biotechnology Information (US); 2012.
4. de Lanerolle NC, Kim JH, Robbins RJ, et al. Hippocampal interneuron loss and plasticity in human temporal lobe epilepsy. *Brain Res* 1989;495:387–395. [PubMed: 2569920]

5. Parent JM, Kron MM. Neurogenesis and Epilepsy. In: th, Noebels JL, Avoli M, Rogawski MA, Olsen RW, Delgado-Escueta AV, editors. *Jasper's Basic Mechanisms of the Epilepsies*. Bethesda (MD) 2012.
6. Pitkanen A, Sutula TP. Is epilepsy a progressive disorder? Prospects for new therapeutic approaches in temporal-lobe epilepsy. *Lancet Neurol* 2002;1:173–181. [PubMed: 12849486]
7. Berg AT, Langfitt J, Shinnar S, et al. How long does it take for partial epilepsy to become intractable? *Neurology* 2003;60:186–190. [PubMed: 12552028]
8. Helmstaedter C, Kurthen M, Lux S, et al. Chronic epilepsy and cognition: a longitudinal study in temporal lobe epilepsy. *Ann Neurol* 2003;54:425–432. [PubMed: 14520652]
9. Kotulska K, Kwiatkowski DJ, Curatolo P, et al. Prevention of Epilepsy in Infants with Tuberous Sclerosis Complex in the EPISTOP Trial. *Ann Neurol* 2021;89:304–314. [PubMed: 33180985]
10. Grabenstatter HL, Del Angel YC, Carlsen J, et al. The effect of STAT3 inhibition on status epilepticus and subsequent spontaneous seizures in the pilocarpine model of acquired epilepsy. *Neurobiol Dis* 2014;62:73–85. [PubMed: 24051278]
11. Hristova M, Rocha-Ferreira E, Fontana X, et al. Inhibition of Signal Transducer and Activator of Transcription 3 (STAT3) reduces neonatal hypoxic-ischaemic brain damage. *J Neurochem* 2016;136:981–994. [PubMed: 26669927]
12. Oliva AA Jr., Kang Y, Sanchez-Molano J, et al. STAT3 signaling after traumatic brain injury. *J Neurochem* 2012;120:710–720. [PubMed: 22145815]
13. Li YZ, Zhang L, Liu Q, et al. The effect of single nucleotide polymorphisms of STAT3 on epilepsy in children. *Eur Rev Med Pharmacol Sci* 2020;24:837–842. [PubMed: 32016989]
14. Hixson KM, Cogswell M, Brooks-Kayal AR, et al. Evidence for a non-canonical JAK/STAT signaling pathway in the synthesis of the brain's major ion channels and neurotransmitter receptors. *BMC Genomics* 2019;20:677. [PubMed: 31455240]
15. Lund IV, Hu Y, Raol YH, et al. BDNF selectively regulates GABAA receptor transcription by activation of the JAK/STAT pathway. *Sci Signal* 2008;1:ra9. [PubMed: 18922788]
16. Riffault B, Medina I, Dumon C, et al. Pro-brain-derived neurotrophic factor inhibits GABAergic neurotransmission by activating endocytosis and repression of GABAA receptors. *J Neurosci* 2014;34:13516–13534. [PubMed: 25274828]
17. Ben Haim L, Ceyzeriat K, Carrillo-de Sauvage MA, et al. The JAK/STAT3 pathway is a common inducer of astrocyte reactivity in Alzheimer's and Huntington's diseases. *J Neurosci* 2015;35:2817–2829. [PubMed: 25673868]
18. Kwon SH, Han JK, Choi M, et al. Dysfunction of Microglial STAT3 Alleviates Depressive Behavior via Neuron-Microglia Interactions. *Neuropsychopharmacology* 2017;42:2072–2086. [PubMed: 28480882]
19. Reichenbach N, Delekate A, Plescher M, et al. Inhibition of Stat3-mediated astrogliosis ameliorates pathology in an Alzheimer's disease model. *EMBO Mol Med* 2019;11:e9665. [PubMed: 30617153]
20. Deacon RM. Measuring motor coordination in mice. *J Vis Exp* 2013:e2609. [PubMed: 23748408]
21. Shiotsuki H, Yoshimi K, Shimo Y, et al. A rotarod test for evaluation of motor skill learning. *J Neurosci Methods* 2010;189:180–185. [PubMed: 20359499]
22. Buettner C, Poci A, Muse ED, et al. Critical role of STAT3 in leptin's metabolic actions. *Cell Metab* 2006;4:49–60. [PubMed: 16814732]
23. Schmued LC, Hopkins KJ. Fluoro-Jade B: a high affinity fluorescent marker for the localization of neuronal degeneration. *Brain Res* 2000;874:123–130. [PubMed: 10960596]
24. Schmued LC, Hopkins KJ. Fluoro-Jade: novel fluorochromes for detecting toxicant-induced neuronal degeneration. *Toxicol Pathol* 2000;28:91–99. [PubMed: 10668994]
25. Kashani A, Lepicard E, Poirel O, et al. Loss of VGLUT1 and VGLUT2 in the prefrontal cortex is correlated with cognitive decline in Alzheimer disease. *Neurobiol Aging* 2008;29:1619–1630. [PubMed: 17531353]
26. Oni-Orisan A, Kristiansen LV, Haroutunian V, et al. Altered vesicular glutamate transporter expression in the anterior cingulate cortex in schizophrenia. *Biol Psychiatry* 2008;63:766–775. [PubMed: 18155679]

27. van der Hel WS, Verlinde SA, Meijer DH, et al. Hippocampal distribution of vesicular glutamate transporter 1 in patients with temporal lobe epilepsy. *Epilepsia* 2009;50:1717–1728. [PubMed: 19389151]
28. Sloviter RS, Zappone CA, Harvey BD, et al. Kainic acid-induced recurrent mossy fiber innervation of dentate gyrus inhibitory interneurons: possible anatomical substrate of granule cell hyperinhibition in chronically epileptic rats. *J Comp Neurol* 2006;494:944–960. [PubMed: 16385488]
29. Sutula T, He XX, Cavazos J, et al. Synaptic reorganization in the hippocampus induced by abnormal functional activity. *Science* 1988;239:1147–1150. [PubMed: 2449733]
30. Chi ZH, Wang X, Cai JQ, et al. Zinc transporter 3 immunohistochemical tracing of sprouting mossy fibres. *Neurochem Int* 2008;52:1305–1309. [PubMed: 18406010]
31. Ivashkiv LB, Donlin LT. Regulation of type I interferon responses. *Nat Rev Immunol* 2014;14:36–49. [PubMed: 24362405]
32. Tsai MH, Pai LM, Lee CK. Fine-Tuning of Type I Interferon Response by STAT3. *Front Immunol* 2019;10:1448. [PubMed: 31293595]
33. Hu Y, Lund IV, Gravielle MC, et al. Surface expression of GABAA receptors is transcriptionally controlled by the interplay of cAMP-response element-binding protein and its binding partner inducible cAMP early repressor. *J Biol Chem* 2008;283:9328–9340. [PubMed: 18180303]
34. Brooks-Kayal AR, Shumate MD, Jin H, et al. Selective changes in single cell GABA(A) receptor subunit expression and function in temporal lobe epilepsy. *Nat Med* 1998;4:1166–1172. [PubMed: 9771750]
35. Brooks-Kayal AR, Shumate MD, Jin H, et al. Human neuronal gamma-aminobutyric acid(A) receptors: coordinated subunit mRNA expression and functional correlates in individual dentate granule cells. *J Neurosci* 1999;19:8312–8318. [PubMed: 10493732]
36. Petryshen TL, Middleton FA, Tahl AR, et al. Genetic investigation of chromosome 5q GABAA receptor subunit genes in schizophrenia. *Mol Psychiatry* 2005;10:1074–1088, 1057. [PubMed: 16172613]
37. Raud S, Sutt S, Luuk H, et al. Relation between increased anxiety and reduced expression of alpha1 and alpha2 subunits of GABA(A) receptors in Wfs1-deficient mice. *Neurosci Lett* 2009;460:138–142. [PubMed: 19477223]
38. Tsien JZ, Chen DF, Gerber D, et al. Subregion- and cell type-restricted gene knockout in mouse brain. *Cell* 1996;87:1317–1326. [PubMed: 8980237]
39. Bielefeld P, Sierra A, Encinas JM, et al. A Standardized protocol for stereotaxic intrahippocampal administration of kainic acid combined with electroencephalographic seizure monitoring in mice. *Front Neurosci* 2017;11:160. [PubMed: 28405182]
40. Bouillere V, Ridoux V, Depaulis A, et al. Recurrent seizures and hippocampal sclerosis following intrahippocampal kainate injection in adult mice: electroencephalography, histopathology and synaptic reorganization similar to mesial temporal lobe epilepsy. *Neuroscience* 1999;89:717–729. [PubMed: 10199607]
41. Groticke I, Hoffmann K, Loscher W. Behavioral alterations in a mouse model of temporal lobe epilepsy induced by intrahippocampal injection of kainate. *Exp Neurol* 2008;213:71–83. [PubMed: 18585709]
42. Murphy BL, Hofacer RD, Faulkner CN, et al. Abnormalities of granule cell dendritic structure are a prominent feature of the intrahippocampal kainic acid model of epilepsy despite reduced postinjury neurogenesis. *Epilepsia* 2012;53:908–921. [PubMed: 22533643]
43. Arabadzisz D, Antal K, Parpan F, et al. Epileptogenesis and chronic seizures in a mouse model of temporal lobe epilepsy are associated with distinct EEG patterns and selective neurochemical alterations in the contralateral hippocampus. *Exp Neurol* 2005;194:76–90. [PubMed: 15899245]
44. Miltiadous P, Kouroupi G, Stamatakis A, et al. Subventricular zone-derived neural stem cell grafts protect against hippocampal degeneration and restore cognitive function in the mouse following intrahippocampal kainic acid administration. *Stem Cells Transl Med* 2013;2:185–198. [PubMed: 23417642]
45. Levesque M, Avoli M. The kainic acid model of temporal lobe epilepsy. *Neurosci Biobehav Rev* 2013;37:2887–2899. [PubMed: 24184743]

46. Althaus AL, Zhang H, Parent JM. Axonal plasticity of age-defined dentate granule cells in a rat model of mesial temporal lobe epilepsy. *Neurobiol Dis* 2016;86:187–196. [PubMed: 26644085]
47. Chaaya N, Battle AR, Johnson LR. An update on contextual fear memory mechanisms: Transition between Amygdala and Hippocampus. *Neurosci Biobehav Rev* 2018;92:43–54. [PubMed: 29752958]
48. Kim JJ, Fanselow MS. Modality-specific retrograde amnesia of fear. *Science* 1992;256:675–677. [PubMed: 1585183]
49. Marschner A, Kalisch R, Vervliet B, et al. Dissociable roles for the hippocampus and the amygdala in human cued versus context fear conditioning. *J Neurosci* 2008;28:9030–9036. [PubMed: 18768697]
50. Kim WB, Cho JH. Encoding of contextual fear memory in hippocampal-amygdala circuit. *Nat Commun* 2020;11:1382. [PubMed: 32170133]
51. Lalonde R, Bensoula AN, Filali M. Rotorod sensorimotor learning in cerebellar mutant mice. *Neurosci Res* 1995;22:423–426. [PubMed: 7478307]
52. Scholz J, Niibori Y, P WF, et al. Rotarod training in mice is associated with changes in brain structure observable with multimodal MRI. *Neuroimage* 2015;107:182–189. [PubMed: 25497397]

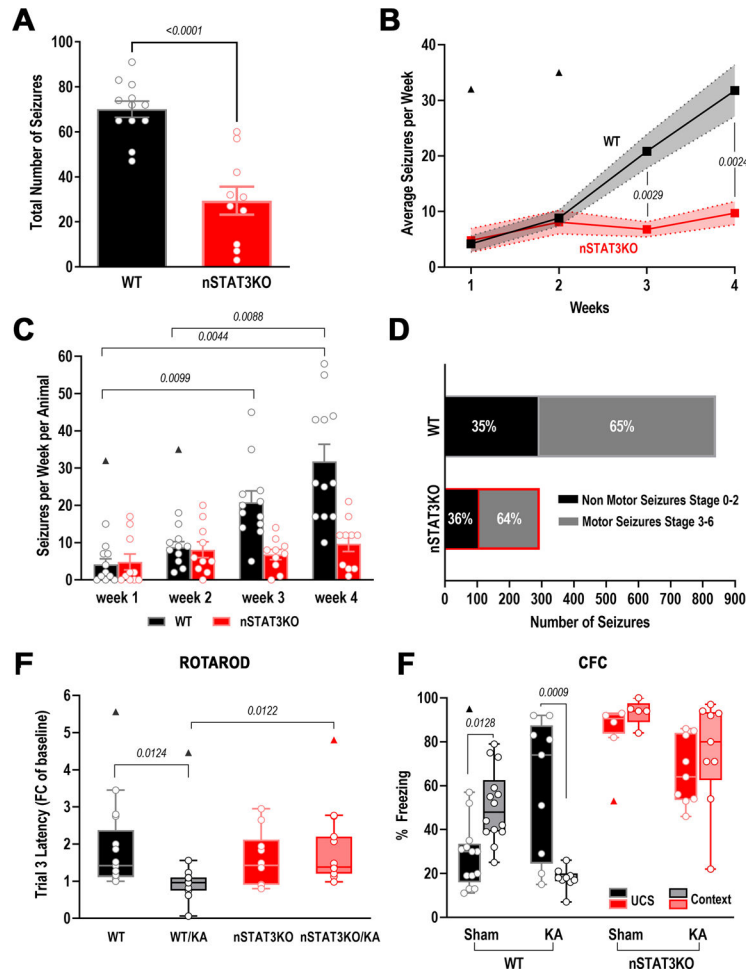


**Figure 1. STAT3 KO reduces SRS frequency and epilepsy progression and improves contextual fear memory and motor learning in epileptic mice.**

The total number of seizures in the 4 weeks after IHKA injection (A) was significantly lower in nSTAT3KO mice compared to WT (Student's unpaired *t*-test). Mean seizures per week (B; shaded areas represent SEM) were significantly lower in IHKA-nSTAT3KO (red; *n* = 10) vs WT (black; *n* = 12) in weeks 3 and 4 after IHKA. Seizure frequency over 4 weeks after IHKA (C; bars represent average) increased in WT but not nSTAT3KO. Statistical analysis was performed by 2-way ANOVA mixed effect model (REML) followed by Šídák's (B) or Tukey's (C) post-hoc tests. Outliers (shown as triangles) were identified with the Grubbs' algorithm and were excluded from the analysis. Proportion of motor seizures (stage 3–6) relative to nonmotor seizures (stage 0–2) recorded in the 4 weeks after KA-induced SE (D) showed no difference between nSTAT3KO (*n* = 10; nonmotor = 107, motor = 187) vs WT mice (*n* = 12; motor = 548, nonmotor = 293; Fisher's exact test). WT group included both mice treated for 5 days with TX (*n* = 6) and mice treated with equal volumes of vehicle (*n* = 6) since TX did not produce any significant changes in any of the EEG outcomes for WT mice (Fig S2). EEG signals were sampled at 2 kHz, amplified 500×, and band-pass filtered between 0.1 Hz and 500 Hz. Electrographic seizures (discriminated from background noise based on large-amplitude [ 3x baseline], high frequency [ 5 Hz], with progression of spike frequency lasting for a 10 s) were

manually detected in EEG recordings and correlated with behavioral manifestations in continuous video recordings utilizing a modified Racine scale.<sup>10</sup> Seizure stages are defined as follows: *stage 0* = electrographic only; *stage 1* = freezing; *stage 2* = head-bobbing, Straub tail; *stage 3* = forelimb clonus; *stage 4* = 4-limb clonus with rearing; *stage 5* = clonus, rearing and falling; *stage 6* = clonus with loss of tone, jumping. Electrographic seizures stage

3 were classified as motor and seizures scored as stage 2 were classified as nonmotor. **E.** Motor learning skills were tested in IHSaline-WT (n = 14), IHKA-WT (WT/KA, n = 14), IHSalinenSTAT3KO (n = 10), and IHKA-nSTAT3KO (nSTAT3ko/KA, n = 12) mice in 3 trials separated by ~5-min intervals. Each mouse was placed on a horizontal rotating cylinder (Med-Associates, model ENV-575M), and tested first with no rotation for 10 s followed by rotation increasing gradually from 3 to 30 rpm over the course of 5 min. Time spent on the rod before falling was recorded. Mice were tested 3 times, with an ~5-min delay between tests. Latencies recorded in Trial 3 were normalized by values obtained in Trial 1 to exclude the contribution of the motor component of the test and assess learning capabilities over time. As data did not display a normal distribution, the Kruskal-Wallis test followed by Dunn's post-hoc was used for multiple comparisons analysis. The Grubbs' method was applied to identify outliers, which were excluded from analysis. A statistically significant difference was observed between IHSaline- and IHKA-WT, and between KA-treated WT and nSTAT3KO, pointing to a KA-dependent impairment of learning abilities over time in WT that was not observed in nSTAT3KO mice. **F.** Contextual fear conditioning (CFC) testing was performed in WT (n = 14) and nSTAT3KO (n=5) mice injected with IHSaline (Sham). Mice in both groups exhibited a behavioral freezing response that was increased 2-min after unconditioned stimulus (UCS) exposure and was retained 48 h later (Context) when placed back in the same context. In IHKA-WT mice (WT/KA, n = 9), epilepsy impaired memory of context (reduced freezing) at the 48-h retention test. In contrast, epileptic nSTAT3KO (nSTAT3KO/KA, n = 11) exhibited retained memory of context (freezing) at 48 h. Percent time spent freezing in response to the UCS, measured during the 2 min after the last shock, is compared to the percent time spent freezing when the same mouse is placed in the same context 48 h later. Only mice exhibiting a freezing rate >10% to the UCS on day 1 were included in the analysis. Statistical analysis was performed using Kruskal-Wallis followed by Dunn's post-hoc test. Outliers (shown as triangles) have been identified with the Grubbs' algorithm and excluded from analysis.

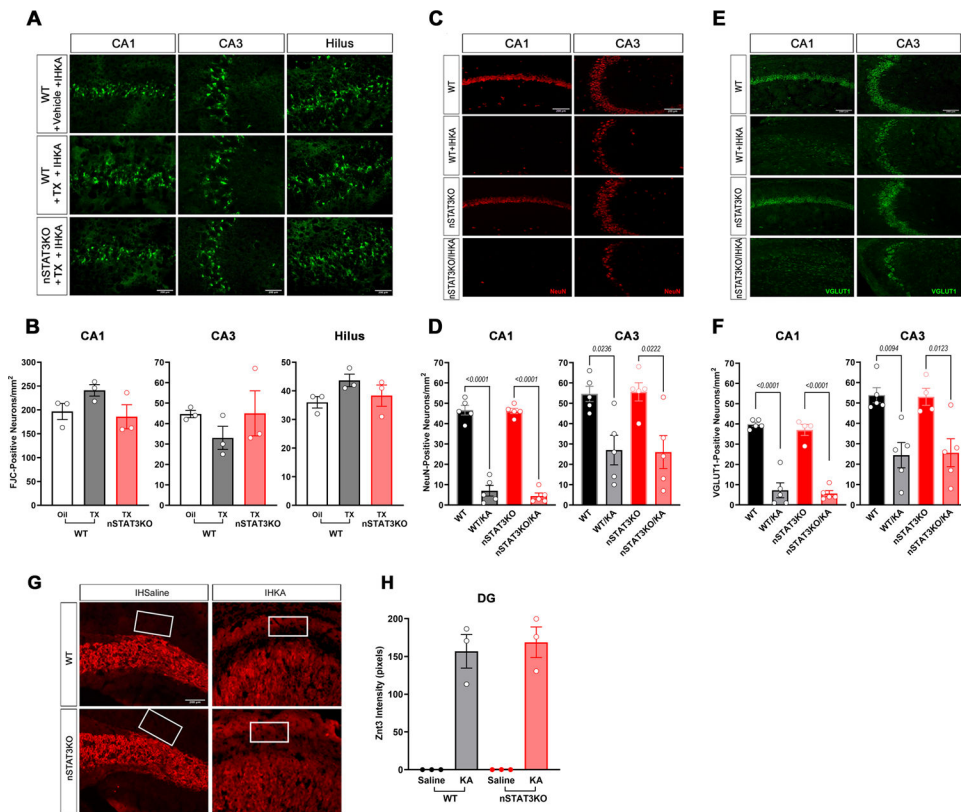


**Figure 2. nSTAT3KO does not protect against IHKA-induced acute or chronic neuronal loss nor mossy fiber sprouting.**

**A-B** Two weeks after TX or vehicle treatment, an IHKA injection was performed in WT/oil, WT/TX, and nSTAT3KO mice ( $n = 3$  mice/group). Mice were killed 48 h after IHKA injection. Fluoro-Jade C (FJC) staining was performed in coronal sections (14- $\mu\text{m}$ , ~8 sections per animal) obtained from all groups. A 1-in-10 series of sections from each brain was processed. Representative images of FJC-stained CA1, CA3, and hilus subregions ipsilateral to the IHKA injection are shown (A). Images were taken at 10X magnification. FJC-positive cells (positively stained cells per  $\text{mm}^2$ ) were counted blindly within standardized areas of the CA1, CA3, and hilar regions of the hippocampus ipsi- and contra-lateral to IHKA or IHSaline injection using ImageJ Analysis software (v. 1.53a). Number of FJC-positive cells in CA1, CA3, or hilus are reported as mean  $\pm$  SEM (B). The mean number of positive cells in each region was calculated from all sections processed for each animal. No statistically significant differences were detected among groups in any of the 3 hippocampal regions tested. Statistical analysis was performed using a 1-way ANOVA, followed by Tukey's post-hoc test. **C-F** Immunofluorescence staining of NeuN (C, D) and VGLUT1 (E, F) was performed in coronal sections (5/mouse, ~1 in 10 series, 5 mice/group) from TX-treated WT and nSTAT3KO mice 5–6 weeks after IHSaline (WT, nSTAT3KO) or IHKA injection (WT+IHKA, nSTAT3KO+IHKA). Representative images of NeuN- and VGLUT1- stained CA1 and CA3 subregions ipsilateral to injection are shown in panels C and E. (contralateral staining shown in Fig S3). Images were acquired using 10X objective on a Nikon Eclipse TE2000-U fluorescence microscope. NeuN-positive cells were manually counted using ImageJ software. Statistically significant reductions in NeuN-positive (D)

and VGLUT-positive (**F**) cells were observed in ipsilateral CA1 and CA3 following IHKA injection (compared to respective saline-treatment) in both WT and nSTAT3KO mice. No significant difference in CA1 or CA3 NeuN-positive or VGLUT-positive cells was detected between WT-IHKA and nSTAT3KO-IHKA. Statistical analysis was performed using 1-way ANOVA followed by Tukey's post-hoc analysis. \* $p < 0.05$  and \*\*\*\* $p < 0.0001$ . **G-H**. Brains from TX-treated WT and nSTAT3KO mice were collected 5–6 weeks after IHSaline (controls) or IHKA injections, fixed by perfusion with 4% PFA and sectioned (14- $\mu$ m coronal). Sections were stained with anti-ZnT3 antibody (~5 sections/mouse, 3 mice/group). Images of ZnT3 staining in the inner molecular layer (IML) above the upper blade of DGCs and ipsilateral to IHSaline or IHKA injection were obtained with a Nikon Eclipse TE2000-U fluorescence microscope at 10X magnification (**G**). Fluorescence intensity was quantified with ImageJ on 16 bit-converted images. The white squares demarcate the area used for the quantification of ZnT3 immunoreactivity. The area of ZnT3 immunoreactivity was quantified in 3 sections and values averaged to determine the levels of "sprouting" detected in each individual mouse (**H**). Mice injected with saline showed no labeling in the IML while the IHKA-injected mice showed presence of ZnT3 fluorescent staining indicative of mossy fiber sprouting. No statistically significant difference was observed in ZnT3 staining intensity between IHKA-WT (n= 3) and IHKA-nSTAT3KO (n= 3) mice (ANOVA, followed by Tukey's post-hoc test).



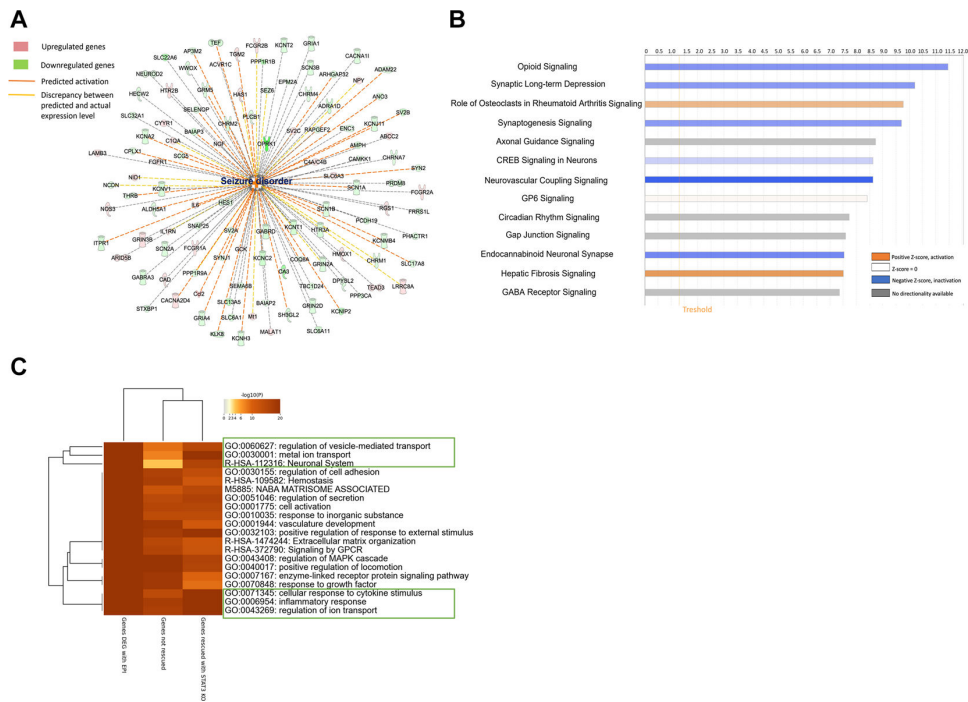


**Figure 4. nSTAT3KO rescues many IHKA-induced alterations in gene expression.** Twenty-four hours after SE, nSTAT3KO rescued the expression changes induced by IHKA. **A.** Enrichment analysis results from the IPA database demonstrate that gene changes seen 24 h after IHKA correspond with gene patterns characteristic of seizure disorder, hence the “Seizure Disorder” node is represented in orange. The directionality shown in the figure shows that nSTAT3 KO rescued many gene expression changes associated with an increased likelihood of seizures. **B** IPA Top Canonical Pathways enriched for in nSTAT3 KO rescued gene set. The directionality represented in the figure corresponds to gene expression changes induced by IHKA injection and absent in nSTAT3KO mice. Thus, among the genes rescued by nSTAT3 KO are the IHKA-induced gene changes associated with decreased synaptic long-term depression (LTD), such that nSTAT3 KO reverses the suppression of LTD otherwise seen in animals 24 h post SE. Results of enrichment analysis for top pathways rescued by nSTAT3 KO using IPA suggest rescue of key pathways related to inflammation (Role of osteoclasts in RA, Hepatic fibrosis) and neuronal function and communication (Opioid signaling, synaptic LTD, Synaptogenesis, Endocannabinoid Neuronal Synapse Pathway, GABA receptor signaling). **C.** nSTAT3KO provides partial rescue of numerous pathways altered by IHKA. Results from concurrent enrichment analysis of IHKA-induced genes, genes not rescued by nSTAT3 KO, and nSTAT3 KO rescued genes in Metascape, demonstrate that nSTAT3 KO partially dampens the expression of many pathways altered by IHKA, rather than selectively and completely rescuing a few pathways. While there are numerous pathways shared among the lists, the processes that are boxed in green, which relate to neuronal signaling and immune system activation, show greater enrichment among the rescued gene dataset, indicating these may be important functions through which STAT3 KO provides rescue after SE. Darker orange bars indicate that there are more genes related to that process in the dataset, which are indicated by significance. Processes or pathways identified by gene enrichment analysis are referred to as “rescued” after nSTAT3 KO in

the IHKA model dependent on whether all genes, or the majority of them, are no longer found within the corresponding gene list. Likewise, processes or pathways that are “partially rescued” represent those where only a portion of the genes are absent indicating that the pathway is still engaged but at a predicted lower level (see also Figs 5–7).

Author Manuscript

Author Manuscript

Author Manuscript

Author Manuscript

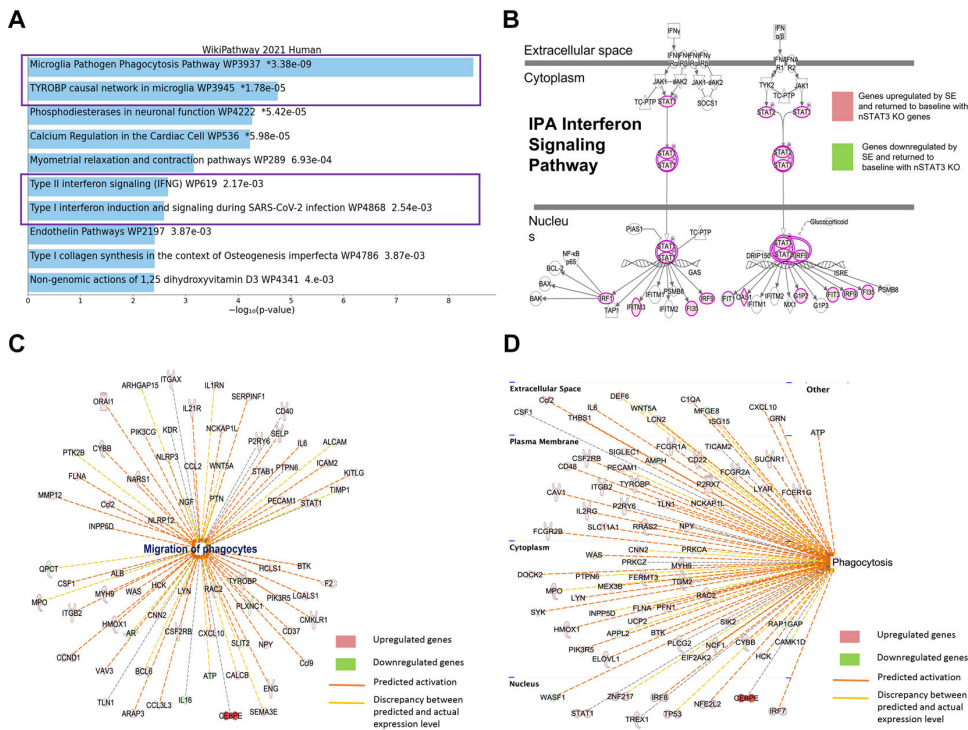


**Figure 5. A potential role for nSTAT3 in brain inflammatory pathways.**

**A.** Top pathways in the WikiPathway 2021 Human database enriched for in the nSTAT3 KO gene rescue lists. These include those related to immune system functioning (boxed in purple), including function and activation of microglial cells, as well as interferon signaling, known to be regulated by JAK/STAT signaling. The blue color of the bars is arbitrary and has no meaning, while bar length reflects the significance value of that pathway among genes rescued with nSTAT3 KO. **B.** nSTAT3 KO rescues many IHKA-induced changes in gene expression relevant to interferon signaling. The directionality represented in the figure corresponds to gene expression changes induced by IHKA, which were then rescued in nSTAT3KO mice. Thus, nSTAT3 KO seems to attenuate the IHKA-associated activation of interferon signaling. **C.** nSTAT3 KO rescues the IHKA-induced increase in genes that promote the migration of phagocytes, including microglia. **D.** nSTAT3 KO rescues IHKA-induced gene alterations that promote increased phagocytic function of immune cells. The directionality represented in panels B, C, and D corresponds to gene expression changes induced by IHKA and rescued in mice with nSTAT3 KO.

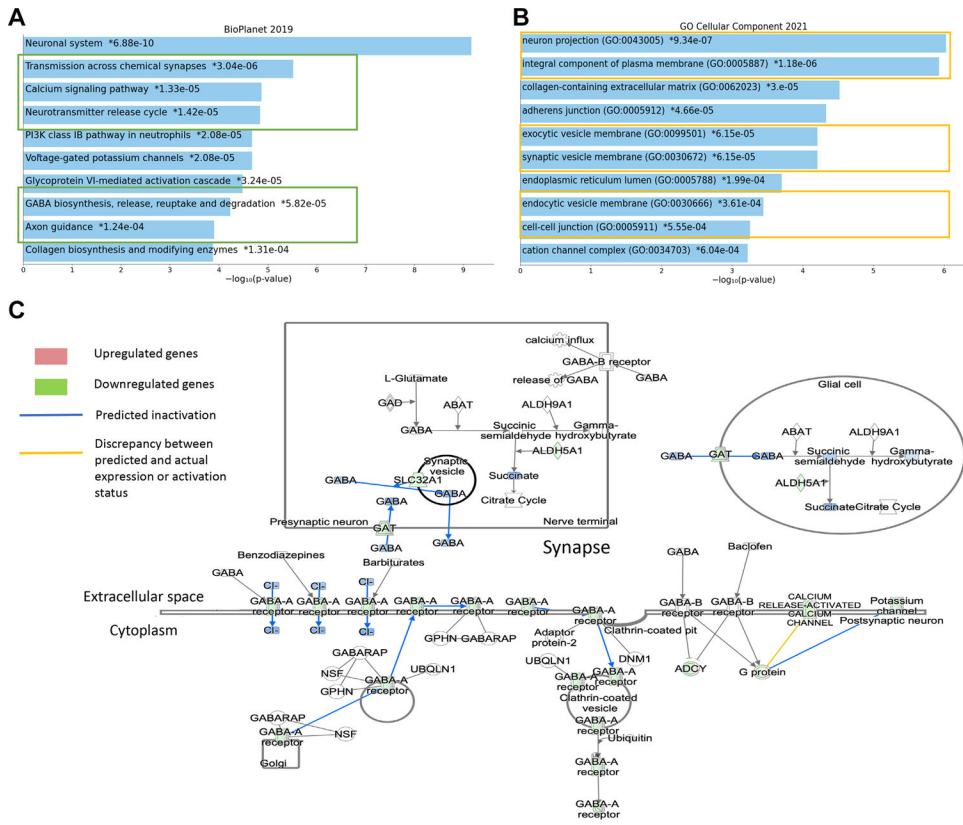


**Figure 6. Pathway enrichment analysis conducted via enrichR revealed that many genes rescued with nSTAT3 KO are related to neuronal signaling and function.**

**A.** The top pathways of the nSTAT3 KO rescue gene set enriched for in the BioPlanet 2019 database are various pathways related to neurotransmission and neuronal functioning (boxed in green), including transmission across chemical synapses; calcium signaling pathway; neurotransmitter release cycle; GABA biosynthesis, release, reuptake and degradation; and axon guidance. **B.** Top cellular compartments enriched for among nSTAT3 KO rescued genes in the GO Cellular Component 2021 database. Many genes rescued with nSTAT3 KO localize to cellular compartments important for neuronal signaling (boxed in yellow), including cell parts essential for neurotransmission such as neuron projection, exocytic vesicle membrane, synaptic vesicle membrane, endocytic vesicle membrane and cell to cell junctions. The color of the bars is arbitrary and has no meaning, while bar length reflects the significance value of that pathway among genes rescued with nSTAT3 KO. **C.** nSTAT3 KO rescues many IHKA-induced gene changes involved in GABAergic signaling. This graphic display, depicting the GABA Signaling canonical pathway from IPA, suggests that many of the gene changes observed 24 h post-IHKA relate to GABAergic signaling, and overall promote a decrease in its function. The directionality represented in the figures corresponds to gene expression changes made by IHKA and reversed in mice with nSTAT3 KO. Thus, nSTAT3 KO rescues the IHKA-associated downregulation of key genes within the GABAergic pathway.

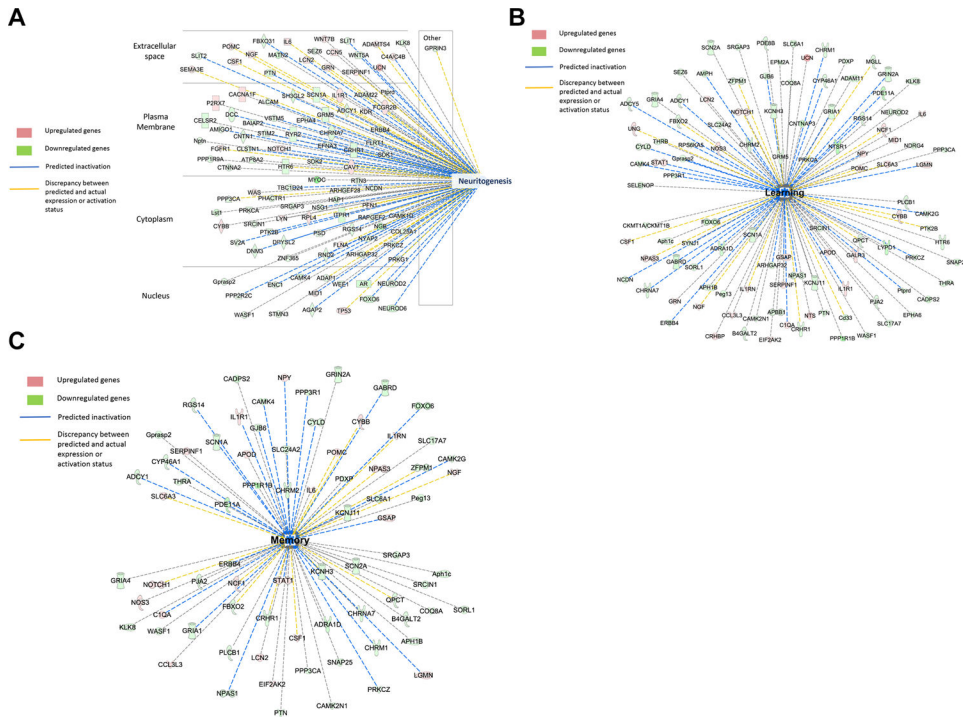


**Figure 7. Predicted functional effect of nSTAT3 KO in synaptic plasticity and behavior.**  
**A.** Enrichment analysis results from the IPA database screen for genes altered 24 h post-IHKA correspond with gene patterns characteristic of a decrease in the production of new neurites, hence, the neuritogenesis node is represented in blue. Thus, nSTAT3 KO rescues many gene expression changes associated with a suppression of neuritogenesis by IHKA. **B** nSTAT3 KO reverses IHKA-induced gene expression alterations associated with decreased learning. IPA enrichment analysis suggests that gene changes observed 24 h post-IHKA correspond with gene patterns characteristic of impaired learning. Thus, nSTAT3 KO rescues many gene expression changes associated with impaired learning induced by IHKA. **C.** nSTAT3 KO rescues IHKA-induced gene expression alterations associated with impaired memory performance. Here, IPA database enrichment analysis demonstrates that gene changes observed 24 h post-IHKA correspond with gene patterns characteristic of impaired memory. The directionality represented in the figures reflects gene expression changes made by IHKA and reversed in mice with nSTAT3 KO. Thus, nSTAT3 KO rescues many gene expression changes associated with impaired memory induced by IHKA.

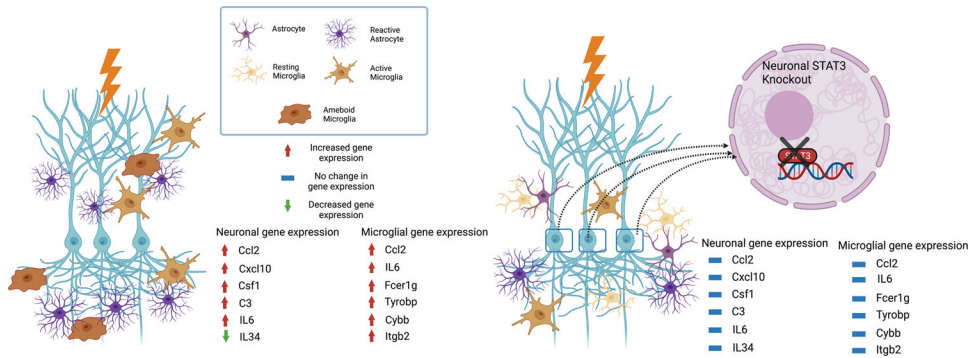


**Figure 8. Proposed model for the hippocampal inflammatory response to brain injury in the presence and absence of neuronal STAT3 function.**

The pictorial representation on the left is the expected response of cells in the hippocampus to a severe acute brain injury like SE (lightning bolt). These brain insults would be expected to induce the upregulation of pro-inflammatory cytokines and attractant molecules in neurons and glial cell types, and to promote the transition of many microglia and astrocytes from a resting to a reactive phenotype, consistent with the early transcriptomic response to IHKA injection seen in the present study (arrows represent the direction of hippocampal gene expression changes between IHKA and saline injection in WT mice 24 h after SE). In contrast, on the right, is a hypothesized representation of the cellular milieu in response to IHKA in the setting of nSTAT3 KO, consistent with the observed normalization (depicted by “-“) of gene expression changes in nSTAT3KO mice as compared with WT mice. Importantly, nSTAT3KO mice express fewer pro-inflammatory genes across numerous cell types despite modification of STAT3 only in neurons. Overall, the dampened pro-inflammatory signature suggests a diminished polarization of astrocytes and microglia to reactive states over the course of disease progression, though some reactive cells likely remain associated, given that nSTAT3KO mice continue to show expression of some pro-inflammatory markers and do not show a rescue of neuronal cell death. Abbreviations: Ccl2, C-C motif chemokine ligand 2; Cxcl10, C-X-C Motif chemokine ligand 10; Csf1, colony stimulating factor 1; C3, caspase 3; IL6, interleukin 6; IL34, interleukin 34; Fcεr1g, Fc epsilon receptor Ig; Tyrobp, transmembrane immune signaling adaptor TYROBP; Cybb, cytochrome b (-245), beta chain; p91, phox; Itgb2, integrin beta 2.